Accepted Manuscript

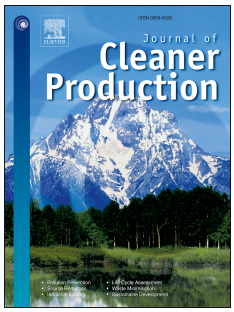

Cost, energy and emissions assessment of organic polymer light-emitting device architectures

Catrice M. Carter, Justin Cho, Aaron Glanzer, Nikola Kamcev, Deirdre M. O'Carroll

PII: S0959-6526(16)31091-5

DOI: 10.1016/j.jclepro.2016.07.186

Reference: JCLP 7758

To appear in: *Journal of Cleaner Production*

Received Date: 11 March 2015

Revised Date: 19 July 2016

Accepted Date: 27 July 2016

Please cite this article as: Carter CM, Cho J, Glanzer A, Kamcev N, O'Carroll DM, Cost, energy and emissions assessment of organic polymer light-emitting device architectures, *Journal of Cleaner Production* (2016), doi: 10.1016/j.jclepro.2016.07.186.

Cost, Energy and Emissions Assessment of Organic Polymer Light-Emitting Device Architectures

Catrice M. Carter,[a] Justin Cho,[a] Aaron Glanzer,[a] Nikola Kamcev,[a] and Deirdre M. O'Carroll*[a,b]

[a]*Dept. of Materials Science and Engineering, Rutgers University, 607 Taylor Rd., Piscataway, NJ 08854, USA*

[b]*Dept. of Chemistry and Chemical Biology, Rutgers University, 610 Taylor Rd., Piscataway, NJ 08854, USA*

**Corresponding author. Tel.: +1 848 445 1496, E-mail address: ocarroll@rutgers.edu (D. M. O'Carroll)*

Graphical abstract

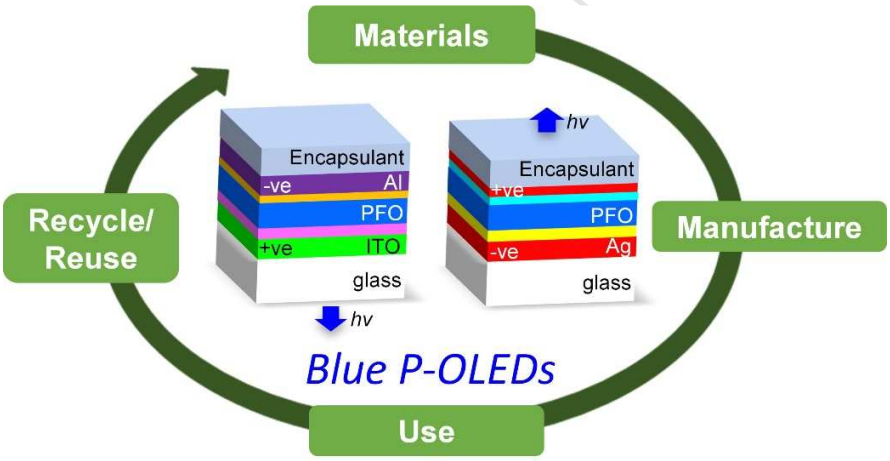

Keywords: polymer OLED; cost; energy; efficiency; life-cycle; greenhouse gas

Total word count: 12 153

Abbreviation	Unit	Definition	Description
lm	-	lumen	SI unit of luminous power
cd	-	candela	SI unit of luminous intensity brightness
W	-	watt	SI unit of power
h	-	hour	Unit of time
d	-	day	Unit of time
a	-	year	Unit of time
kW h	-	kilowatt hour	Unit of energy
C_{dev}	$/m^2	device cost per area	The total cost of materials and cost to manufacture a device architecture with an area of 1 m^2
C_{op}	$/a	yearly operating cost	Cost to operate the device for 8 h/d over a period of 1 a
C_{lm}	$/h	optical power cost	Cost to continuously generate 1000 cd/m^2 for 1 h
$GHG\text{-}CO_{2,dev}$	kg	mass of CO_2 emissions from device production	Mass of CO_2 greenhouse gas emissions from raw materials extraction and manufacturing of a device with an area of 1 m^2
E_{mat}	MJ/kg	material embodied energy	Embodied energy of the raw materials in a device per mass
E_{man}	MJ/kg	direct process energy	Energy consumed during device manufacturing per mass
I_{CO2}	kg/kW h	CO_2 emission intensity	Average CO_2 emission intensity
$GHG\text{-}CO_{2,op}$	kg/a	emission mass flow rate for CO_2	Yearly CO_2 emissions produced from a device with an area of 1 m^2 operating for 8 h/d
C_{mat}	$	cost of materials in the device	Cost of raw materials used for a device with an area of 1 m^2
C_{man}	$	manufacturing cost	Cost to manufacture a device with an area of 1 m^2
C_{use}	$	use phase cost	The cost to electrically power each device architecture
L	h	operational lifetime	The length of time it takes for device luminous efficacy to degrade by 50 %
C_{elec}	$/(kW h)	cost of electricity in the USA	The cost of electricity in the USA per energy
E_{use}	kW h or GJ	use-phase energy consumption	The electrical energy needed to operate a device over its entire use phase
P_{in}	W	power in	Electrical power applied to the device
M_v	lm/m^2	luminous exitance	Light output power emitted by a device

B_f	lm/W	luminous efficacy	Electrical-to-optical power conversion efficiency
k	0.75	correction factor	Accounts for device operation at 75 % of its initial luminous efficacy, on average, due to degradation and efficiency roll-off during its operational lifetime
B	cd/m^2	luminance	Used to quantify the brightness of a light-emitting device per area

16

Abstract

Proponents for sustainable alternative lighting and display options advocate for organic light-emitting diodes (OLEDs), particularly polymer-based organic light-emitting diodes (P-OLEDs), because of their potential for low-cost fabrication, more versatile device formats and lower power consumption compared to traditional options. Here, an economic, energy and CO_2 emissions assessment is carried out for four different laboratory-scale, blue-emitting P-OLED device architectures: bottom-emitting conventional; bottom-emitting inverted; top-emitting conventional; and top-emitting inverted. Additionally, comparisons with a standard, commercial-scale, blue inorganic light-emitting diode (LED) device architecture are made. The various P-OLED device architectures are investigated due to their potential to increase operational lifetime (inverted) and light out-coupling efficiency (top-emitting). The following metrics are used in this assessment: device cost per area, yearly operating cost, optical power cost, CO_2 emissions from device production, and yearly operating CO_2 emissions. We show that the top-emitting inverted device architecture significantly reduces the device cost per area, yearly operating cost, optical power cost and CO_2 emissions for the P-OLED devices, due to elimination of indium tin oxide and its comparatively high luminous efficacy and longer lifetime. In addition, the top-emitting inverted P-OLED device architecture performs competitively at the laboratory scale with commercial-scale inorganic LEDs for all metrics. However, if top-emitting P-OLEDs are to be manufactured on a large scale, the luminous efficacy assumed for laboratory-scale devices needs to remain constant throughout development to remain competitive.

1. Introduction

OLEDs are being investigated as sustainable alternative display and lighting options, as opposed to compact fluorescent lamps, incandescent lighting, and LEDs because of their low temperature growth conditions and potential earth-abundant constituent elements (while organic phosphorescent OLEDs usually contain rare-earth elements to harvest triplet excitons, fluorescent OLEDs have active layers that are primarily composed of carbon and hydrogen). However, current small-molecule OLEDs on the market are fabricated under high vacuum using thermal deposition, thus making the fabrication process expensive [1-9]. Therefore, low-cost, large-scale fabrication options are needed to make OLED technologies more marketable. P-OLEDs are an emerging sub-section of OLED technologies that are more amenable to solution-based processing which may enable more straight-forward, vacuum-free fabrication of the devices and, hence, lower cost and lower process energy consumption [2,10-13].

However, the lower efficiency (i.e., luminous efficacy) and the shorter operational lifetime of blue P-OLEDs compared to red and green P-OLEDs, slows the commercialization of a full-color P-OLED for general lighting and display purposes [2]. The lower efficiency of blue P-OLEDs can be attributed to the difficulty of charge injection into blue-emitting fluorescent polymers which have low highest-occupied molecular orbital (HOMO) energies (ca. –5.9 eV) and high lowest-unoccupied molecular orbital (LUMO) energies (ca. –2.1 eV) [14]. Common approaches that have been used to remedy these issues are incorporation of a high-work-function hole injection layer, such as poly(3,4-ethylenedioxythiophene):poly(styrenesulfonate) (PEDOT:PSS), and a low-work-function electron transport layer, such as calcium (Ca) or lithium fluoride (LiF) into the device structure [15-17]. Additionally, while internal quantum efficiency can be optimal (~100 % for phosphorescent OLEDs and phosphorescent P-OLEDs) [18], light-extraction efficiency is quite low (~20 % to 31 %) [18-20], especially for blue-emitting devices and is a significant barrier to high-efficiency P-OLEDs. The shorter operational lifetime of conventional blue, fluorescent P-OLEDs is due to a combination of: (1) higher drive voltages due to the low light extraction efficiency; (2) corrosion of indium tin oxide (ITO) due to

the acidity of the PEDOT:PSS layer [3,21] and (3) degradation of PEDOT:PSS and Ca carrier injection properties due to exposure to water vapour and oxygen during device fabrication or operation [3].

Proposed approaches to tackling efficiency and operational lifetime issues are: (1) light management approaches, such as use of top-emitting device architectures, and addition of metallic or dielectric nanostructures to promote more efficient light extraction [22]; (2) inverted device architectures [23]; (3) improved encapsulation methods [24]. While these approaches have been shown to have the potential to increase device efficiency and operational lifetime [22-24], they may in turn affect the overall cost and environmental impact. Thus, further assessment of these approaches must be completed before any definitive conclusions can be drawn as to their usefulness. The goal of this study is to carry out an cost, energy and CO_2 emissions assessment, based on life-cycle assessment (LCA) methodologies, for four laboratory-scale, prototypical, fluorescent, blue-emitting P-OLED device architectures (conventional bottom-emitting, inverted bottom-emitting, conventional top-emitting and inverted top-emitting architectures) to determine which architecture is more effective in terms of device cost per area, yearly operating cost, optical power cost, energy consumption, and CO_2 emissions. Additionally, comparisons are made with the more ubiquitous, commercial-scale, blue inorganic LED device. As discussed earlier, the inverted P-OLED architectures increase the operational lifetime and the top-emitting P-OLED architectures increase the electrical-to-optical power conversion efficiency (i.e., luminous efficacy) [3,8,23].

Several economic and LCA studies have been conducted for LEDs and organic photovoltaic (OPV) devices which form the basis of our study for P-OLEDs [4-7,25-39]. A case study for the LCA of LED downlight luminaires concluded that the environmental impact of LEDs is dominated by the use-stage energy consumption and data gaps exist in LED product manufacturing and its environmental impacts; thus, resulting in a need for further research and assessments in order to compare LED-based luminaires with existing lighting technologies [28]. The U. S. Department of Energy has carried out detailed LCAs of energy and environmental impacts of LED lighting products, which show that the average life-cycle energy consumption is similar for both compact fluorescent lamps and LEDs, with it

being greater for incandescent lamps [7]. While economic, energy and environmental assessments have been completed for inorganic LEDs not much emphasis has been placed on the organic counterpart, which motivates this study. We draw comparisons with polymer-based OPV device economic and LCA studies, where applicable, since there have been a significant number of such studies [4-6,22,27-39] and, while OLEDs and OPV devices are operationally different, their device compositions and architectures are similar. As a result, one can study prior work on OPVs in order to draw inspiration to base future organic polymer-based cost and LCA studies due to the similarities in device structure and material type with the main difference being that polymer-based OPV devices produce electrical energy from sunlight while P-OLEDs consume electrical energy to produce light.

Furthermore, numerous OPV studies have focused on identifying approaches to lower device cost and the effects of increasing the efficiency and operational lifetime on energy and greenhouse gas (GHG) emission metrics that are also pertinent to P-OLEDs. For example, a life-cycle and cost assessment of OPV devices by Emmott et al. explored various transparent conductor alternatives to ITO in which they found that material alternatives, such as silver nanowires and high-conductivity PEDOT:PSS, have the potential to reduce the energy-payback time (EPBT) and financial cost of organic photovoltaic devices [4]. Espinosa et al. conducted a LCA of organic tandem solar cells where they investigated the economic and environmental feasibility of manufacturing a tandem solar cell versus a single junction solar cell. They found that the tandem solar cell has to be 20 % better performing than a single-junction device in order to improve cost and sustainability metrics [27]. A review paper by Lizin et al. of LCA studies of OPVs focused on environmental aspects such as cumulative energy demand (CED), EPBT, and the GHG emission factor of single-junction, organic, bulk-heterojunction P3HT:$PC_{60}BM$ polymer-based solar cells [5]. The top environmentally performing solar cell had a CED of 37.58 MJ/m^2, EPBT from 3.54 months to 6.24 months, and cell efficiency of 2 % with lower GHG emission factors than current power plants. They concluded that the often-used linear relationship between increasing operational lifetime or efficiency and improved sustainability, CED and EPBT, is not a sufficient model because improvements in these areas are heavily dependent on the device materials and architectures [5]. Darling et al. conducted

a LCA to estimate the CO_2 emission factor for a OPV device with an area of 1 m^2, with 1 % solar power conversion efficiency (PCE) and one year operational lifetime (which are achievable today), and a hypothetical future OPV device with 15 % PCE and a 20 year operational lifetime [6]. They estimated a ~10 % decrease in CO_2 emissions due to the increase in PCE and the longer operational lifetime. Furthermore, they suggest that improvements can be made to operational lifetime through encapsulation with materials with low water and oxygen transport rates and use of air-stable alternative materials. Additionally, in order to transfer OPV technology from laboratory-scale to larger scales for commercialization, efficiency, scalability of manufacturing processes, and knowledge of degradation mechanisms and their impacts on operational lifetime are critical factors that have been identified through economic and LCA studies [5,6,29-39].

The aforementioned OPV studies allow us to draw some conclusions that are applicable to P-OLED devices, such as: eliminating ITO from the device architectures, increasing multilayer device performance, and use of stable device materials and encapsulants should assist in making P-OLED performance more comparable with the performance of current LEDs on the market. However, comparisons between certain aspects such as life-cycle CO_2 emissions and cost assessments of photovoltaic devices and light-emitting devices are not appropriate or straight forward. For example, once a photovoltaic system is installed, the main yearly cost is associated with system maintenance, while, for a lighting system there are significant additional costs because it consumes electricity during operation (as opposed to generating electricity from a free natural resource, i.e. the sun, as in the case of a photovoltaic system). Therefore, in our study we develop some alternative assessment methodologies and metrics that are relevant to P-OLED devices but not to OPV devices.

2. Methodology

2.1 Goal and Scope

As mentioned in Section 1, the goal of this study is to carry out a cost, energy and CO_2 greenhouse gas (GHG-CO_2) emissions assessment, based on LCA methodologies, for four laboratory-scale, prototypical, fluorescent, blue-emitting P-OLED device architectures to determine which architecture is more effective in terms of device cost per area, yearly operating cost, optical power cost, energy consumption, and CO_2 emissions. LCA is used as a tool to assess the energy and environmental impacts of a product, process or activity throughout its life cycle; from the extraction of raw materials through to processing, transport, use and disposal [4,5,7,25-42]. LCA is a standard international ISO 14040 series method that consists of four distinct components: (1) goal and scope, (2) inventory analysis, (3) impact assessment, and (4) interpretation. First, the aim of the study, central assumptions, and system boundaries are chosen. Next, during the life-cycle inventory analysis (LCI) phase, the inputs and outputs for the emissions and resources are quantified. Then a life cycle impact assessment (LCIA) is conducted to evaluate the potential environmental impact of the previous quantified values. Finally, an interpretation of results are presented in a clear concise manner [27,41,42].

We complete cradle-to-grave assessment, i.e., from the inception of raw materials to the end of use, of a fluorescent, blue-emitting P-OLED device (i.e., one that uses, for example, a polyfluorene-based light-emitting active layer) as there are numerous results reported in the literature for such devices [1,3,8-14]. As discussed in Section 1, while photovoltaic studies can be used as a guide to base LCA studies of light-emitting devices on, they differ in terms of their operation. Unlike OPVs, P-OLEDs consume electrical power for operation and produce optical power (i.e., light). As a result, the functional unit should be determined by the basis of the optical power produced, which in our case we are assuming to be the brightness per area or luminance. Therefore, here, we employ a luminance of 1000 cd/m^2 as our functional unit which is a commonly reported luminance for OLEDs [2,24,43-50]. Each device architecture is assumed to produce this constant brightness, and in order for this to be achieved either the electrical input power or the power efficiency (i.e., luminous efficacy) of the device can be varied. Note that in contrast, for OPV devices a constant optical input power (or irradiance) is applied during performance testing (i.e., 100 mW/cm^2 (1 sun)); therefore, to generate a particular target electrical power

quantity, device area or efficiency is varied. We determine the following metrics: the device cost per area, including materials and manufacturing costs; yearly operational cost; cost to continuously generate 1000 cd/m^2 for one hour; and the GHG-CO_2 emissions, for both device production and yearly operation, from the point of view of the user. The assessment carried out here is meant to provide perspective on the cost, energy and emissions impact of blue-emitting P-OLEDs relative to the more mature inorganic semiconductor LED technologies. Additionally, the P-OLED life-cycle stages and materials which are expected to have the greatest cost and emissions impacts are identified.

2.2 Central Assumptions

In this study, we completed a cradle-to-grave assessment including the following stages (Fig. 1): (1) raw materials extraction and production; (2) PLED device fabrication and (3) PLED device use. The following inputs and outputs are considered for each stage where relevant: material inputs; electrical energy inputs; GHG-CO_2 emissions outputs and optical energy output, and P-OLED device use stages. A life-cycle inventory is compiled and analyzed for the materials, production and fabrication, and use-phase operating cost of the PLEDs in order to carry out the assessment. In our assessment, we ignore all transport, installation, and disposal phase costs associated with the life-cycle of the P-OLED because these costs are assumed to be small compared to device and use-phase costs [4,31,40]. Furthermore, we have not included in the assessment the housing, electrical connections, heat sinks, or others items involved in the mounting of the P-OLED as it is assumed to be similar amongst the different P-OLED architectures regardless of the final product (e.g., lighting, display) because they are all planar, thin-film surface-emitting optoelectronic devices and our functional unit (i.e., 1000 cd/m^2) is the same for each architecture. Conversely, for the inorganic LED different housing, mounting and peripheral components (e.g., electrical connections, heat sinks) could certainly be employed. However, given that the blue inorganic LED is the most ubiquitous blue light-emitting device, it is useful as a standard against which blue OLEDs can be compared (similar to how a silicon solar cell is the standard against which all newer solar cell technologies are compared regardless of eventual differences in mounting, housing, etc. [6]).

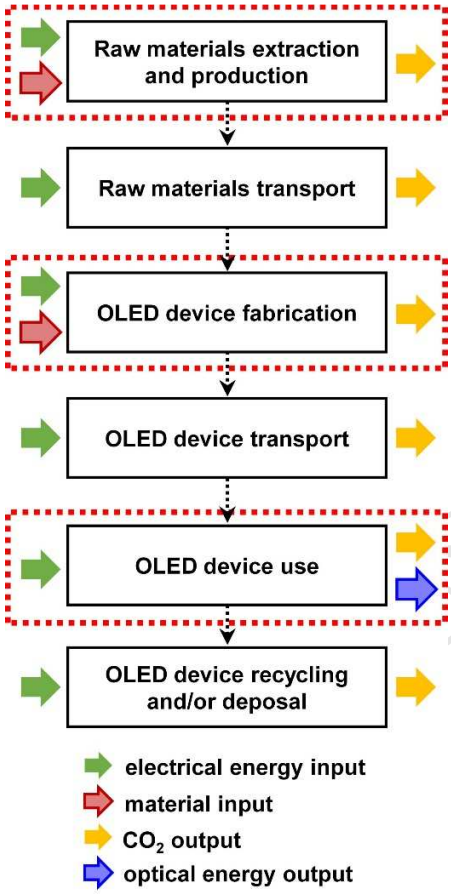

Fig. 1. System boundary diagram for a LCA of OLEDs. In this study, our assessment considers only the stages of the life cycle highlighted in by the dashed red boxes: raw materials extraction and production, OLED device fabrication, and OLED device use.

Our background system (i.e., the information needed to carry out this study) is defined through extensive reviews of published literature and supplier catalogues. Embodied energy and direct process energy values were obtained from published literature that included relevant embodied energy data from LCA databases such as Ecoinvent and Gabi for the more common materials (e.g., glass, silver). However, in some cases, material embodied energy values were assumed values based on more commonly-available materials within the same material class. For example, material embodied energies for poly(3-hexylhiophene) were used instead of those for poly(9,9-dioctylfluorene)), PFO, for the organic conjugated polymer active layer due to lack of available embodied energy data for PFO. This is a reasonable approach because both P3HT and PFO are conjugated (i.e., semiconducting) polymers that have rigid

molecular backbones that consist of molecular monomers or long chains of carbon-based repeat units connected by covalent bonds. In addition, both polymers are synthesized from a solution in a similar catalytic fashion [51,52]. The cost per mass data for materials were obtained from supplier online catalogues and from published literature. References to the source websites (including date accessed) and the relevant papers are included at the appropriate location for each cost per mass value. For the thickness of layers in the different P-OLED devices (Tables 1 and 2), information was obtained from published literature in which device prototypes were fabricated and tested, as well as Department of Energy solid-state lighting technical reports (referenced below).

The performance parameters (Table 3) are essential to calculating the metrics defined in Section 2.3 used for the assessment of the different device architectures, which comprise our foreground system. Note that only lab-scale and pilot-scale fluorescent blue polymer OLED devices have been reported to date. Therefore, all of our metrics for the OLED devices are for lab/pilot-scale devices. First, the average operational lifetimes of conventional blue fluorescent OLEDs were determined from references [2,43,44]. Then, based on publications in which direct comparisons between the lifetime of a conventional and inverted OLED were made [45,46], a scaling factor was determined. From this assessment we found that the inverted OLEDs have operational lifetimes that are 1.75 times longer than the conventional OLEDs. We then multiplied the average conventional operational P-OLED lifetime by the scaling factor to determine the inverted OLED operational lifetimes for both bottom and top emitting device structures.

The luminous efficacy values were calculated in a similar fashion to the operational lifetime. To determine the luminous efficacy values for the different device architectures, first, we averaged the luminous efficacy values for conventional bottom emitting fluorescent blue OLEDs from references [10,44,52] at a luminance of 1000 cd/m^2. Then, in a similar way to how the operational lifetime of the inverted devices was determined, a scaling factor was taken from reports that directly compared inverted to conventional bottom emitting OLEDs [45,54-57], top emitting to bottom emitting conventional OLEDs [58], and the top emitting to bottom emitting inverted OLEDs [56,59-61]. We then used these scaling factors to calculate the efficacy values from the averaged conventional bottom emitting OLED luminous

efficacy for each device configuration. Note that the luminous efficacy value of the inorganic LED was based on reported values for mass-produced inorganic LEDs that included light extraction structures and housing [48,50,62-65], which may aid in increasing efficacy values.

2.3 Definition of Metrics

Our metrics for this assessment are as follows: (1) device cost per area, C_{dev}, which is the upfront cost to the user at the initial purchase; (2) yearly operating cost, C_{op}, which is the cost to operate the device for 8 h/d over a period of one year; (3) optical power cost, C_{lm}, which is the cost required to generate the functional unit of 1000 cd/m^2 of optical power for one hour; (4) GHG-CO_2 emissions from raw materials extraction and device manufacturing, $GHG\text{-}CO_{2,dev}$; (5) yearly GHG-CO_2 emissions produced from a device operating for 8 h/d, $GHG\text{-}CO_{2,op}$. We define C_{dev} as:

$$C_{dev} = C_{mat} + C_{man} \qquad (1)$$

where C_{mat} is the materials cost for all device layers and C_{man} is the manufacturing cost. Estimation of C_{mat} for each device architecture studied here will be discussed in the next section using information obtained from materials suppliers and is the largest contribution to C_{dev}.

C_{man} is determined from a percentage range of the total device costs reported for solution-processed OPV device manufacturing costs on the lab/pilot scale, i.e., 21 % to 40 % [6,27,29-51]. Note due to the current state of P-OLED development, large-scale manufacturing methods and practices are currently not optimized or standardized. Additionally, comparisons between manufacturing costs for reel-to-reel processed devices and manufacturing costs for devices fabricated on ridged substrates have shown only a slight increase in the percentage contribution of manufacturing costs to total device costs (~50 % is an upper estimate for OPV devices on glass substrates compared to 21 % to 40 % for OPV on PET substrates). Therefore, we have assumed an average percent contribution of manufacturing costs to total device costs of 30 % [6,27,29-51]. Therefore, to determine C_{man}, such that C_{man} contributes to 30 % of

C_{dev}, C_{man} was taken to be a 43 % of C_{mat}. We do not account for possible differences in manufacturing costs between lighting and display P-OLED technologies such as types of capital equipment (e.g., spray coaters versus ink-jet printers). However, in both cases the active layer, hole transport layer (HTL) and ETL are assumed to be fully solution processed on glass [11,12]. Additionally, as stated earlier, this study focuses on device costs per area; costs associated with (P-O)LED housing, electrical connections, heat sinks and electronic drivers (i.e., balance of system costs) are not included.

We define C_{op} as:

$$C_{op} = \frac{C_{use}}{L} * 8 * 365 \qquad (2)$$

where L is the operational lifetime of the device and C_{use} is the use-phase cost. L is taken to be the time it takes for the luminous efficacy to drop to 50 % of its initial value [68]. C_{use} is the cost of operation for a device (with area of 1 m^2) over the device's operational lifetime and is defined as:

$$C_{use} = C_{elec} * E_{use} \qquad (3)$$

where C_{elec} is taken to be the cost of electricity in the United States (assumed to be 0.0984 \$/(kW h) [69]), and E_{use} is the use-phase energy consumption defined as:

$$E_{use} = \frac{P_{in} * L}{1000} \qquad (4)$$

where P_{in} is operating electrical power for a device with an area of 1 m^2. P_{in} is calculated as follows:

$$P_{in} = \frac{M_v}{B_f}\, k \qquad (5)$$

where B_f is the luminous efficacy and k is a correction factor, which accounts for the performance degradation of the device over time. Here, we assume a constant applied voltage is applied to each device, therefore, k = 0.75 (i.e., on average, the device operates at 75 % of its initial luminous efficacy over its operational lifetime, L) [68]. M_v is the luminous exitance (i.e., the light output power) and is defined as

$$M_v = B * \pi \qquad (6)$$

where B is luminance which we have taken to be 1000 cd/m^2, as discussed earlier in Section 2.1, as it is the standard value used when reporting operational lifetimes of OLED devices [2,24,41-50]. We assume C_{lm} in \$/h is then calculated as:

$$C_{lm} = \frac{M_v * C_{elec}}{B_f * 1000}. \qquad (7)$$

Next, CO_2 emissions from device production, $GHG\text{-}CO_{2,dev}$, which includes the GHG-CO_2 emissions from raw materials and device fabrication in kg of CO_2 is defined as:

$$GHG\text{-}CO_{2,dev} = (E_{mat} + E_{man}) * I_{CO2} \quad (8)$$

where E_{mat}, in MJ/m^2, is the embodied energy of the raw materials in the devices and E_{man}, in MJ/m^2, is the direct process energy consumed during device manufacturing. E_{man}, which is taken to be 1.05 times E_{mat}, is determined from averaged ratios of direct process energy to embodied energy in the material from relevant OPV literature [27,29-31]. The average CO_2 emission intensity from fossil fuels, I_{CO2}, between 1997 and 2012 for the United States from electricity generation is taken to be 1.90 kg/(kW h) of CO_2 (equal to 0.53 kg/MJ of CO_2) [70]. Finally, the emission mass flow rate for CO_2, $GHG\text{-}CO_{2,op}$, which is the yearly GHG-CO_2 emission produced from a device (area of 1 m^2) operating 8 h/d (in kg/a of CO_2) is defined as:

$$GHG\text{-}CO_{2,op} = \frac{(E_{use} * I_{CO2} * 8 * 365)}{L} \qquad (9)$$

3. Life-Cycle Inventory - Device Architectures and Materials

The bottom-emitting conventional P-OLED was analysed initially as a foundation with which to compare the bottom-emitting inverted, the top-emitting conventional and the top-emitting inverted P-OLED architectures, and the blue inorganic LED. Schematics of the different P-OLED architectures and the inorganic LED are shown in Fig. 2a-e.

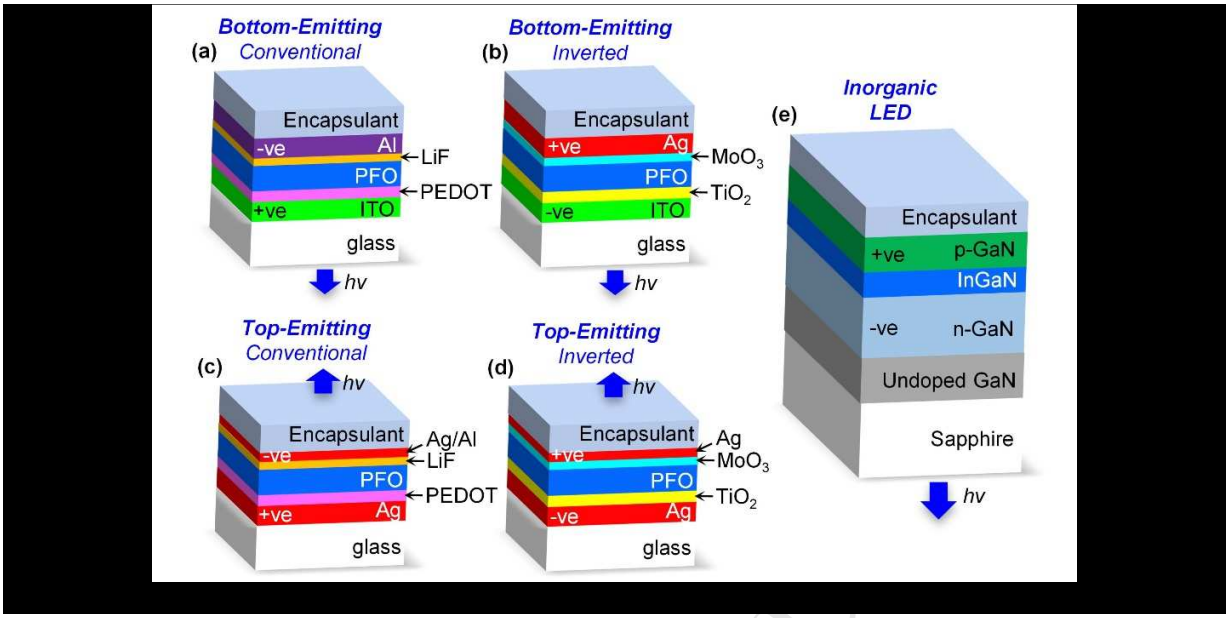

Fig. 2. Schematics of: (a) a bottom-emitting conventional P-OLED, (b) a bottom-emitting inverted P-OLED, (c) a top-emitting conventional P-OLED, (d) a top-emitting inverted P-OLED, and (e) a blue inorganic LED. The blue arrows with *hv* (photon energy) labels represent the direction of light emission.

The inventory of materials and average layer thicknesses for each device architecture, obtained from published literature, is included in Table 1.

Table 1. Table of bottom-emitting (conventional and inverted) and top-emitting (conventional and inverted) P-OLED device layer materials, layer thicknesses and corresponding layer functions. The thickness values are an average of values reported in the corresponding referenced literature with the standard deviation shown after the average value. Glass substrates with thickness of 0.192 mm were assumed for all P-OLED device architectures.

Device Architecture	Thickness (nm)	Function	References
Bottom-Emitting Conventional			
ITO	108 ± 50	Anode	[4,22,50]
PEDOT:PSS	57 ± 13	HTL	[4,22,52,71-75]
PFO	108 ± 45	active layer	[4,22,50,72-76]
LiF	2.3 ± 2	ETL	[4,71,76]
Al	142 ± 53	Cathode	[4,22,50,73,74,76]
Bottom-Emitting Inverted			
ITO	108 ± 50	Cathode	[4,22,50]
TiO_2	45 ± 40	ETL	[77,78]
PFO	108 ± 45	active layer	[4,22,50,72-76]
MoO_3	11 ± 7	HTL	[8,50,77-84]
Ag	35 ± 30	Anode	[82-84]
Top-Emitting Conventional			

Ag	125 ± 29	Anode	[8,58,85]
PEDOT:PSS	57 ± 13	HTL	[4,22,52,71-75]
PFO	108 ± 45	active layer	[4,22,50,72-76]
LiF	2.3 ± 2	ETL	[4,71,76]
Al	2	Cathode	[85]
Ag	17.8 ± 2.17	Cathode	[8,85]
Top-Emitting Inverted			
Ag	125 ± 29	Cathode	[8,58,85]
TiO_2	45 ± 40	ETL	[77,78]
PFO	108 ± 45	active layer	[4,22,50,72-76]
MoO_3	11 ± 7	HTL	[8,50,77-84]
Ag	17.8 ± 2.17	Anode	[8,85]
Blue Inorganic LED			
sapphire	10^6	substrate	[86,87]
undoped GaN	600	buffer layer	[86,87]
n-doped GaN	1500	ETL	[86,87]
p-doped GaN	500	HTL	[86,87]
InGaN	200	emitter layer	[86,87]

4. Cost Assessment

4.1 Device Cost Per Area

To determine the C_{dev}, we first carried out materials cost calculations to determine C_{mat} using the mass per area for each layer of the device and material cost per mass as shown in Table 2. Using the data obtained from Table 2, the estimated cost for each layer per area (C_A) in a device was calculated as follows:

$$C_A = m * C_m \qquad (10)$$

where m is the mass per area and C_m is the cost per mass of the material in each layer of the device.

Table 2. The mass of each layer for a device (area of 1 m^2), the material cost per mass values and the cost per layer in a particular device are represented for bottom-emitting conventional P-OLED, bottom-emitting inverted P-OLED, top-emitting conventional P-OLED, top-emitting inverted P-OLED, and blue inorganic LED architectures [88-97]. Only the materials that are used in a particular device architecture are represented in the respective column. The cost per layer for the encapsulant is a generic value take from Ref. [32]. Each material layer function is represented by the following superscript characters: $^{\wedge}$substrate, $^{\#}$anode, $^{\times}$HTL, $^{+}$active layer, $^{\sim}$ETL, *cathode.

Materials	Mass per area (g/m^2)	Cost per mass ($/g)	Cost per layer ($/m^2)				
			Bottom-Emitting P-OLED		Top-Emitting P-OLED		Inorganic LED
			Conventional	*Inverted*	*Conventional*	*Inverted*	
Glass$^{\wedge}$	474.24	0.09	42.92	42.92	42.92	42.92	-
ITO	0.73 ± 0.34	114	83.68 ± 38.53$^{\#}$	83.68 ± 38.53*	-	-	-
Al* (142 nm)	0.38 ± 0.14	0.24	0.09 ± 0.03	-	-	-	-
Al* (2 nm)	0.005	0.24	-	-	0.001	-	-
Ag$^{\#}$ (35 nm)	0.37 ± 0.32	6.39	-	2.35 ± 2.01	-	-	-
Ag (17.8 nm)	0.19 ± 0.02	6.39	-	-	1.19 ± 0.15*	1.19 ± 0.15$^{\#}$	-
Ag (125 nm)	1.31 ± 0.30	6.39	-	-	8.38 ± 1.94$^{\#}$	8.38 ± 1.94*	-
PEDOT:PSS$^{\times}$	0.06 ± 0.01	9.02	0.52 ± 0.12	-	0.52 ± 0.12	-	-
$MoO_3$$^{\times}$	0.05 ± 0.03	10.84	-	0.57 ± 0.36	-	0.57 ± 0.36	-
PFO^{+}	0.11 ± 0.05	391	43.79 ± 18.38	43.79 ± 18.38	43.79 ± 18.38	43.79 ± 18.38	-
LiF$^{\sim}$	0.01 ± 0.005	31.30	0.19 ± 0.16	-	0.19 ± 0.16	-	-
$TiO_2$$^{\sim}$	0.19 ± 0.17	3.16	-	0.59 ± 0.53	-	0.59 ± 0.53	-
Sapphire$^{\wedge}$	398	0.52	-	-	-	-	206.96
GaN	15.99	17.55	-	-	-	-	280.62
GaN^{+}	0.86	17.55	-	-	-	-	15.11
InN^{+}	0.41	188	-	-	-	-	76.89
Encapsulant	-	-	11.49	11.49	11.49	11.49	11.49
C_{mat} ($/m^2)	-	-	**182.68 ± 57.22**	**185.39 ± 59.81**	**108.48 ± 20.75**	**108.93 ± 21.36**	**591.07**

By adding the estimated price for each layer (calculated using Equation 10) we determined the estimated C_{mat} of a device with an area of 1 m^2 (excluding manufacturing costs) for each architecture: 183 $/$m^2$ ± 57 $/m (bottom-emitting conventional); 185 $/m ± 60 $/m (bottom-emitting inverted); 108 $/m ± 21 $/m (top-emitting conventional); 109 $/m ± 21 $/m (top-emitting inverted); and 591 $/m (inorganic blue LED). In this way the contribution of each layer to the overall C_{mat} amount for each device could be examined.

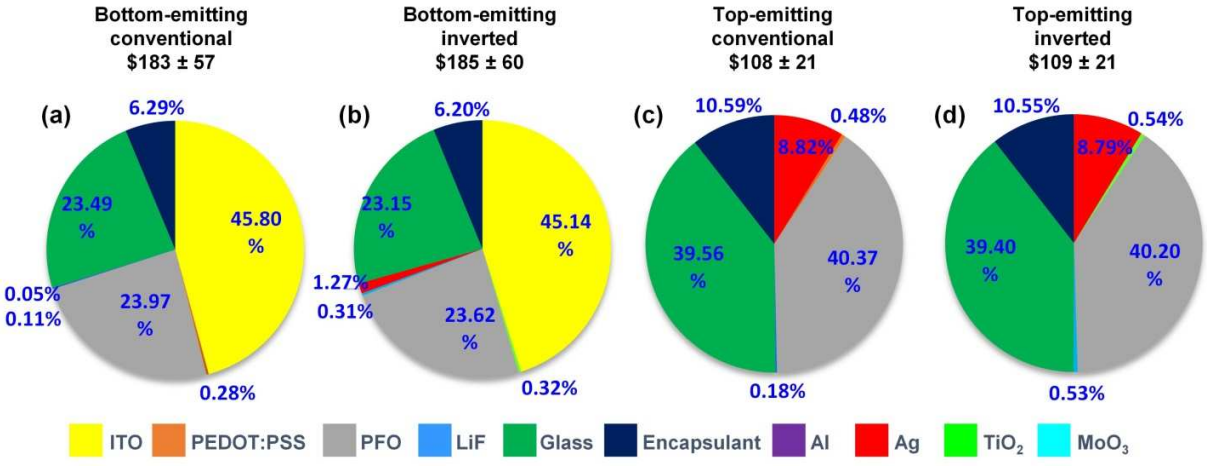

Fig. 3. The percentage cost for each layer in the: (a) bottom-emitting conventional P-OLED; (b) bottom-emitting inverted P-OLED; (c) top-emitting conventional P-OLED; and (d) top-emitting inverted P-OLED. The materials cost, C_{mat}, for each device (area of 1 m^2) is shown above the corresponding pie chart (i.e., manufacturing costs, C_{mat}, not included).

As shown in Figure 3 the ITO, PFO and glass layers contributed the most to C_{mat} for bottom-emitting P-OLEDs (approximately 45 %, 24 % and 23 %, respectively) and the PFO and glass layers contributed the most to C_{mat} for top-emitting P-OLEDs (both ~ 40 %). Despite layer thicknesses of only ~100 nm for both ITO and PFO (Table 1) they were the most expensive materials, per mass, hence the significant percentage contribution to C_{dev}. Conversely, glass was one of the cheapest materials per mass; however, it was also the thickest layer (0.192 mm) which resulted in the significant overall cost per area. The metal layers (Ag and Al) accounted for less than 9 % of the total cost of the materials in the devices. The ETL and HTL layers were negligible in cost compared to the other layers. As a result, there was very little change in cost on going from a conventional to an inverted device architecture. However, since the top-emitting architectures eliminated ITO, the value of C_{mat} was reduced by ~41 % compared to the bottom-emitting devices. C_{mat} is 591 \$/m for the blue inorganic LED device architecture (1 m^2 device), with C_{mat} calculated in a similar fashion to the P-OLED architectures (see Fig. 2 and Table 1). Therefore, C_{mat} for the blue inorganic LED was 5.4 times more than that of the top-emitting P-OLED architecture. This makes the top-emitting architecture a viable option in terms of C_{mat} for solid-state lighting or display applications. C_{dev}, which included a material cost, C_{man}, that was calculated as a percentage of C_{mat} (43 %) such that C_{man} contributed to 30 % of C_{dev} (see Section 2.3), was then determined and the assessment of C_{dev} is included in Section 4 below.

4.2 Use-Phase Cost

We now determine the performance data (operational lifetime and luminous efficacy) obtained from the literature for each device architecture (Table 3) and how much it would cost to electrically power each architecture in the United States (cost of electricity of 0.0984 \$/(kW h)[69]) over the useful life of each device, i.e., the use-phase cost (C_{phase}) using Equations 3-6.

Table 3. The operational lifetime, L, and luminous efficacy, B_f, are represented for the bottom-emitting conventional P-OLED, bottom-emitting inverted P-OLED, top-emitting conventional P-OLED, top-emitting inverted P-OLED and blue inorganic LED.

Performance Parameters	Bottom-Emitting P-OLED		Top-Emitting P-OLED		Inorganic LED	Sources
	Conventional	Inverted	Conventional	Inverted		
L (h)	16 000	28 000	16 000	28 000	50 000	[2,24,41-46,50]
B_f (lm/W)	2.5	3.8	5.1	7.8	7.5	[10,44-65]

As shown in Table 3 the inverted P-OLED architecture has an approximately 75 % longer operational lifetime than the conventional P-OLED architecture (9.6 years compared to 5.5 years, assuming the P-OLED device operated for 8 h/d). The top-emitting inverted device is the most energy efficient of all of the devices (luminous efficacy of 7.8 lm/W), and consumes at least 1.5 times less power that the other P-OLED architectures during operation. However, the blue inorganic LED has a factor of 1.8 longer operational lifetime than the longest operating P-OLED (17.1 years for the inorganic LED). Using the operational lifetime and luminous efficacy values reported in Table 3 along with Equations 3-6, the use-phase cost (C_{phase}) for each architecture was determined; see Figure 4.

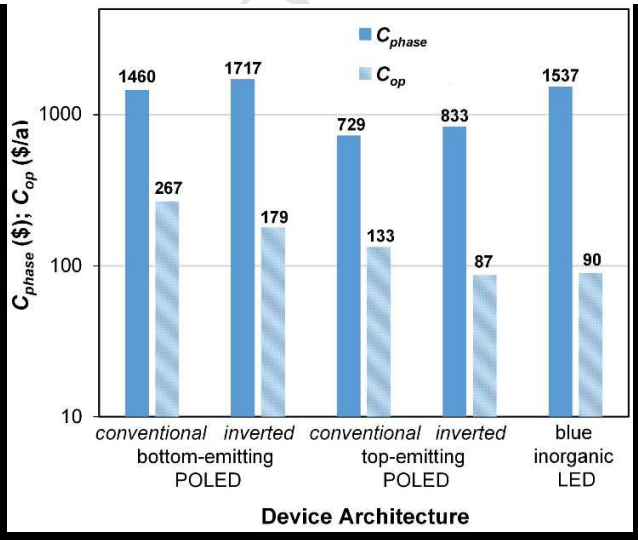

Fig. 4. The corresponding C_{use} and C_{op} values for each P-OLED device architecture and a blue inorganic LED.

We find that the bottom-emitting inverted P-OLED device had the highest use-phase cost (1717 $; see Fig. 4) of all of the devices and the top-emitting conventional device had the lowest use-phase cost of the P-OLED devices (2.4 times smaller than the bottom-emitting inverted architecture) primarily due its higher luminous efficacy and shorter operational lifetime (Table 3). The use-phase cost of the blue inorganic LED was ~2.1 times greater than the top-emitting conventional P-OLED (729 $ and 1537 $, respectively) primarily due to its longer operational lifetime (50 000 h). When the use-phase cost is normalized by the device operational lifetime, we obtain C_{op}, the yearly operating cost, for each device (Fig. 4). The top-emitting inverted P-OLED had the lowest operating cost of all P-OLEDs (261 $/a) and cost 8 $/a lower than the blue inorganic LED (269 $/a) due to the higher luminous efficacy of the former (7.8 lm/W).

4.3 Economic Impact

The following metrics are presented in Table 4 for light-emitting devices with areas of 1 m^2: C_{dev}, C_{op} and C_{lm}. C_{dev} (i.e., including materials and manufacturing costs) was the lowest for the top-emitting P-OLEDs and was approximately 5 times cheaper than the blue inorganic LED.

Table 4. The metrics C_{dev}, C_{op} and C_{lm}, for each P-OLED device architecture and the blue inorganic LED (device areas are 1 m^2 in all cases).

Device Architectures	C_{dev} ($/m^2)	C_{op} ($/a)	C_{lm} ($/h)
Bottom-emitting Conventional P-OLED	261 ± 82	267	0.12
Bottom-emitting Inverted P-OLED	265 ± 85	179	0.08
Top-emitting conventional P-OLED	155 ± 30	133	0.06
Top-emitting Inverted P-OLED	156 ± 31	87	0.04
Inorganic LED	844	90	0.04

This indicates that the top-emitting P-OLEDs are the most attractive device type in terms of up-front costs to the user. The top-emitting inverted P-OLED had the lowest C_{op} of all of the devices due to its high

luminous efficacy (Fig. 4), while the bottom-emitting conventional P-OLED had the highest C_{op}. For C_{lm}, the top-emitting conventional architecture (0.04 $/lm) was the best performing of the P-OLEDs and cost the same as the blue inorganic LED. In short, the top-emitting inverted P-OLED is the most promising P-OLED device architecture in terms of total cost because: (1) it eliminates one of the most expensive layers (ITO) in the device composition; and (2) it has high luminous efficacy in comparison to the other P-OLED device architectures. Furthermore, while the top-emitting P-OLED architecture has a slight advantage over the blue inorganic LED in terms of C_{op}, it is significantly cheaper in terms of C_{dev} (~5 times cheaper). Therefore, even considering the longer lifetime of the inorganic LED (1.8 times longer), the top-emitting P-OLED would still have a lower total cost when factoring in lifetime and replacement device costs (neglecting P-OLED housing and light extraction structures).

5. Energy and CO_2 Emissions Assessment

5.1 Device Embodied Energy

Powering light-emitting optoelectronic devices is tied to GHG emissions through the indirect production of CO_2 during electricity consumption. Furthermore, GHG emission is linked to the use-phase energy of the P-OLED devices, which is expected to be the most significant energy-consumption stage of the P-OLED life-cycle. As referenced in the Department of Energy study on lighting technology it has been shown that the use phase is the largest contributor to the overall energy consumption of such devices as fluorescent, incandescent, and LED lamps [7]. To illustrate this point, we determined the embodied energy, E_{mat}, in P-OLED devices (areas of 1 m^2) using literature values for the embodied energy of each constituent layer material and the mass of each layer of the device (Table 5).

Table 5 Embodied energy in MJ/kg of materials in P-OLED devices.

Materials	Embodied Energy (MJ/kg)	Source
ITO	355 753	[30,31]
PEDOT:PSS	131	[30,33]
PFO*	1843	[30,33]

LiCl[#]	220	[103]
Al	171	[25]
Ag	128	[104]
MoO_3	80	[33]
TiO_2	118	[33,104,105]
Glass	16	[25]
Encapsulant (1 m^2)	10[‡]	[31]

[*]Data for P3HT used here as an approximation for PFO (PFO embodied energies not available), [#]LiCl used here instead of LiF as embodied energy data was limited for LiF; [‡]value is in units of MJ/m^2

As can be seen in Table 5, ITO and PFO have the highest embodied energies 355 753 MJ/kg and 1843 MJ/kg, respectively. We then accounted for the mass of each layer in each P-OLED architecture (Table 6).

Table 6. Embodied energy (in MJ) from raw material extraction per layer of material in P-OLED devices with areas of 1 m^2 (direct layer process energy not included).

Layer	**Bottom-Emitting P-OLED**		**Top-Emitting P-OLED**	
	Conventional	***Inverted***	***Conventional***	***Inverted***
ITO	45.89	45.89	-	-
PEDOT:PSS	0.008	-	0.008	-
PFO	0.207	0.207	0.207	0.207
LiCl[#]	0.001	-	0.001	-
Al	0.078	-	-	-
Ag	-	0.047	0.192	0.192
MoO_3	-	0.004	-	0.004
TiO_2	-	0.022	-	0.022
Glass	39.52	39.52	39.52	39.52
Encapsulant	9.96	9.96	9.96	9.96
Total (E_{mat})	**95.67**	**95.65**	**49.90**	**49.93**

The resulting embodied energies for P-OLED devices (areas of 1 m^2) were ~96 MJ and ~50 MJ for the bottom-emitting and top-emitting P-OLEDs, respectively. The major contribution to the larger bottom-emitting device embodied energy was ITO, making up approximately 48 % of the embodied energy. The other layers that exhibited significant embodied energies were the glass and encapsulant layers (~39 MJ and 10 MJ, respectively); however, these were still significantly smaller than the ITO embodied energy (which was almost 46 MJ). Additionally, the embodied energies of all P-OLED devices were approximately an order of magnitude smaller than the embodied energy estimated for the inorganic

LED (4650 MJ from Ref. 25). However, the total device embodied energy (E_{mat}) for each P-OLED architecture was substantially lower than the use-phase energy (E_{use}; converted to GJ by multiplying its value in kW h by 0.0036) which ranged from 53.4 - 62.8 GJ for the bottom-emitting P-OLEDs, was a value of 26.7 GJ for the top-emitting conventional P-OLED, and was 30.5 GJ and 56.2 GJ for the top-emitting inverted P-OLED and the blue inorganic LED, respectively. Therefore, lowering the use-phase energy should have the greatest effect on reducing environmental impacts caused by energy consumption during operation of the P-OLEDs.

5.2. GHG-Carbon Footprint

The CO_2 emissions from device production, $GHG\text{-}CO_{2,dev}$, were calculated for the four different architectures and the blue inorganic LED using Equation 8 and the embodied energies for raw material extraction shown in Table 6. In addition, $GHG\text{-}CO_{2,op}$, was calculated using Equation 9 and the devices' luminous efficacy and operational lifetime values from Table 3. Both metrics are displayed graphically in Fig. 5.

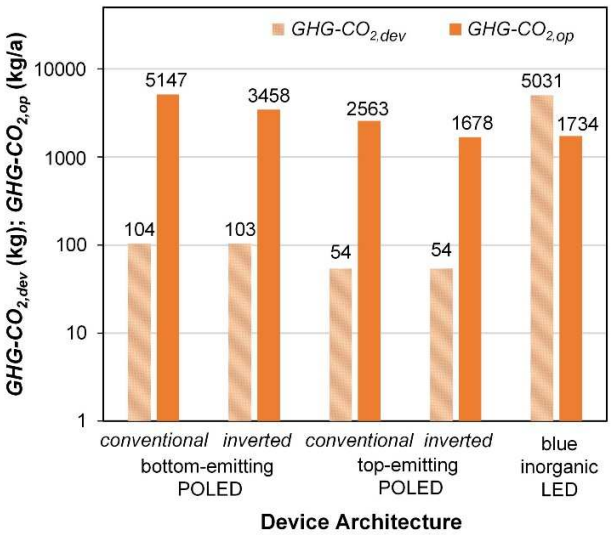

Fig. 5. The corresponding GHG-CO_2 emissions for raw material extraction and device (1 m^2) manufacturing ($GHG\text{-}CO_{2,dev}$) and yearly GHG-CO_2 emissions from operation ($GHG\text{-}CO_{2,op}$) for each P-OLED device architecture and the blue inorganic LED.

The $GHG\text{-}CO_{2,dev}$ is the lowest for the top-emitting P-OLEDs (54 kg of CO_2) due to the low embodied

462 energy for the top-emitting architecture (Table 6). The blue inorganic LED had a substantially higher
463 $GHG\text{-}CO_{2,dev}$ (5031 kg of CO_2) compared to all of the P-OLED devices due to the large amount energy
464 embodied in the materials and the correspondingly high direct process energy. The $GHG\text{-}CO_{2,op}$ was
465 lowest for the top-emitting inverted and blue inorganic LED devices (~1678 kg/a of CO_2 and ~1734 kg/a
466 of CO_2 respectively) because they are more efficient at converting electrical input power to light (Table
467 3). The top-emitting inverted P-OLED produced approximately 67 % less CO_2 during operation than the
468 bottom-emitting conventional P-OLED. Therefore, the top-emitting inverted is the most promising P-
469 OLED architecture for maintaining a low carbon footprint.

470 The post-use environmental effects of both P-OLEDs and inorganic LEDs also need to be
471 considered; however, materials toxicity and degradation, as well as materials recycling, are complex and
472 relatively underdeveloped topics in the context of optoelectronic devices. As a result, data is lacking on
473 the environmental impacts and embodied energy associated with processes being used or under
474 development for disposing of or recycling advanced electronic materials [98]. However, metals can be
475 recycled from both types of devices (including indium, tin, silver, gallium and aluminium) either directly
476 or as a by-product [100]. Costs of purifying the recycled metals is likely to be a compounding issue.
477 Furthermore, it has been shown for OPV the glass substrate can be removed and reused with almost no
478 difference in efficiency, and the polymer layers can biodegrade without leaving harmful elements in the
479 environment [34]. While it would be ideal to recycle the P-OLED and LED devices; the energy required
480 to recycle should be considered. Typically, the energy required to recycle a material is less than that for
481 production of the virgin material [25]. All else being equal, based on the embodied energy (Table 6), the
482 energy required to recycle the inorganic LED (4650 MJ) would still be significantly greater than that of
483 the P-OLEDs (~50-96 MJ) which would make the P-OLED devices the more sustainable choice.

484 Although recycling removes some of the contaminants; unfortunately, optoelectronic devices
485 (recycling rate of 10 %) are not recycled at the same rate as other hazardous consumer products (recycling
486 rate of 24 % to 90 %) [99], and large amounts of optoelectronic materials and devices still end up in
487 landfills or recycling centers where they can adversely affect human health and the environment due to

leeching and evaporation of hazardous substances such as heavy metals [101]. The actual amount of hazardous materials depends on the type of optoelectronics, but as a result of these health and environmental risks governmental agencies have begun to regulate optoelectronic recycling [102].

6. Interpretation, Scenario Analysis and Conclusions

6.1. Interpretation

While improvements in the operational lifetime of P-OLEDs must be made to be competitive with the comparatively long operational lifetime of inorganic blue LEDs, the top-emitting inverted P-OLED device architecture appears to be the most promising device in terms of projected electrical-to-optical power efficiency, with a high luminous efficacy of 7.8 lm/W compared to the 7.5 luminous efficacy for the inorganic blue LED. Furthermore, the device costs per area of P-OLEDs were between 3-5 times cheaper than inorganic LED device costs per area, which would make P-OLED devices more immediately appealing. The embodied energy in the blue inorganic LED was significantly higher than that for all P-OLED device architectures. However, since the embodied energy was only a small fraction (~0.2 % for P-OLEDs and 8 % for the inorganic blue LED) of the use-phase energy of each P-OLED device, the use-phase was deemed to be the most critical stage to focus on to reduce energy consumption and environmental impacts associated with GHG-CO_2 emissions.

6.2. Scenario Analysis

The above interpretation compares laboratory small-scale prototype P-OLEDs to commercial-scale (i.e., mass-produced) blue inorganic LEDs with the P-OLEDs are already cheaper in terms of C_{dev}, and it is likely to remain the case during scale-up of device fabrication. However, OLED large-scale fabrication methods are not well developed and need to be further refined. One of the current obstacles to widespread commercialization of OLEDs is their overall high cost due to small-scale manufacturing and use of ridged substrates and vacuum deposition methods during the OLED or P-OLED device fabrication.

In order to produce P-OLEDs on a large scale and at low cost, the rigid substrate would need to be replaced with a flexible substrate like polyethylene terephthalate (PET) to enable reel-to-reel processing, materials wastage would need to be decreased, and material types and processing methods would need to be revaluated. For example, the glass substrate contributed ~25 % and ~44 % (bottom-emitting and top-emitting, respectively) to the C_{mat} and if it was replaced with PET, assuming a thickness of 0.143 mm [31,35,108], and at a cost of ~0.16 $/g, the C_{mat} for each device would be reduced by approximately 6 % and 10 %, respectively [32]. Furthermore, flexible substrates extend the range of applications for P-OLEDs into not only lighting and standard display options, but also such markets as wearable electronics. In addition, the U.S. Department of Energy estimates that the material utilization rate is as low as 30 % for vapour deposition and as high as 90 % for solution deposition fabrication [9]. In this study, we did not consider fully solution-based fabrication of all layers, thus the deposition of certain layers (e.g., the metal and ITO) by vacuum methods would result in high amounts of materials wastage and increase our predicated C_{dev}. If we account for wastage, C_{dev} is 548 $/m ± 384 $/m and 561 $/m ± 225 $/m for the conventional and inverted bottom-emitting P-OLED architectures, respectively; which represent a factor of 2.1 more than without wastage. However, C_{dev} for the top-emitting device architecture does not increase as significantly when wastage is accounted for because most layers are solution processed (i.e., ITO is eliminated) with C_{dev} increasing only by a factor of 1.25 (to 195 $/m ± 41 $/m) for the top-emitting conventional and inverted device architectures.

Fully solution processed fabrication of P-OLEDs would require alternative material choices to some of those listed in Table 1-2. For example, bulk silver would need to be replaced with silver ink. This alternative material would not have much effect on the overall price as the silver layer(s) do not contribute significantly to C_{dev}; see Fig. 3. However, full solution processing would only be possible for the top-emitting devices due to the vacuum deposition needed for deposition of ITO for conventional P-OLED devices. In addition, for fully-solution-processed, large-scale production the cost of the materials would decrease by a factor of 2, at least, compared to those reported in Table 2 (resulting in C_{mat} between

537 63 $/m^2 and 123 $/m^2 for the bottom-emitting P-OLED and between 44 $/m^2 and 65 $/m^2 for the fully-
538 solution-processed top-emitting P-OLED) because of the bulk purchase of material from the suppliers
539 [32-38]. These estimates are on target with estimates reported by Azzopardi et al., Powell et al. and others
540 for the total device cost of a commercial-scale OPV module which ranges from 45 $/m^2 to 264 $/m^2 [32-
541 38].

542 When addressing the scalability of OLEDs, changes to device luminous efficacy and operational
543 lifetime are important considerations. Large-scale production is likely to yield devices with lower
544 luminous efficacy and operational lifetimes compared to those for small-scale prototypes, due to the
545 increased likelihood of non-uniformities over large active areas as a result of defects, layer thickness
546 variations and/or electrical shorts [39,109]. Reductions in luminous efficacy, in particular, are expected to
547 increase the yearly operating cost of these P-OLED devices. While it is expected that there will be a
548 reduction in both luminous efficacy and operational lifetime due to large-scale production, P-OLEDs are
549 currently manufactured at the lab- and pilot-scale which makes quantification of the reduction in
550 performance difficult. Therefore, in order to estimate the efficiency and lifetime reduction caused by
551 large-scale production, we draw comparisons with reports on the commercial scale-up of OPVs. Lab-
552 scale efficiencies for optimized polymer-based OPVs have been reported to be between 10 % and 12 %
553 (fully solution processed and vacuum evaporated) and OPV modules produced using large-scale
554 processing methods are approximately 2 % efficient; thus indicating in a factor of up to 6 reduction in
555 efficiency during scale-up [38,39,109]. Consequently, assuming a similar reduction in the luminous
556 efficacy for the top-emitting, inverted P-OLED, luminous efficacy would be reduced to 1.3 lm/W for a
557 device fabricated using large-scale production methods.

558 Furthermore, we can assume a worst-cast operational lifetime of 1 year based on prior studies of
559 OPV devices fabricated by large-scale production methods [29,110-112]. This assumption would reduce
560 the top-emitting inverted P-OLED operational lifetime by a factor of 9.6 (i.e., to 2920 h). To illustrate the
561 effect of assuming such significant reductions in luminous efficacy and operational lifetime under a
562 “worst-case” large-scale production scenario, we carried out a scenario analysis using the Monte-Carlo

method for a top-emitting P-OLED where we calculate probability distributions for C_{op}, E_{use} and $GHG\text{-}CO_{2,op}$ under three different scenarios (Fig. 6), assuming relative standard deviations of the luminous efficacy and operational lifetime of 25 % [29,112-118].

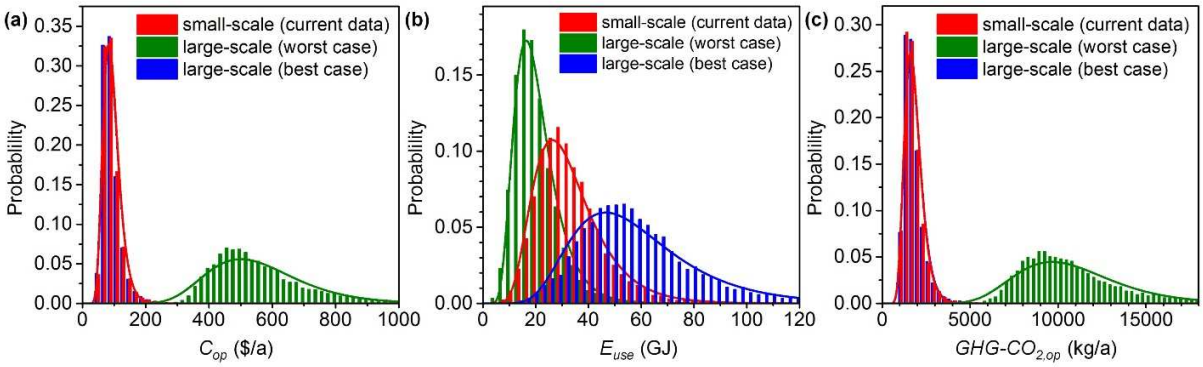

Fig. 6. Histograms showing the probability distribution of (a) C_{op}, (b) E_{use} and (c) $GHG\text{-}CO_{2,op}$ for top-emitting inverted P-OLEDs (1 m^2) generated using the Monte-Carlo method [29] for three different scenarios: small-scale, which assumes luminous efficacy (B_f) and operational lifetime (L) values of 7.9 lm/W and 28 000 h (as reported in Table 3); large-scale (worst case), which assumes a factor of 6 reduction in B_f compared to the small-scale scenario and a 2920 h operational lifetime (i.e., 1 year); and large-scale (best case), which assumes a future "best case" large-scale production scenario that results in P-OLEDs with B_f and L values of 7.9 lm/W and 50 000 h, respectively. Normal distributions for B_f and L were generated as inputs for the Monte-Carlo analysis, assuming a relative standard deviation of 25 % in B_f and L to represent typical performance parameter variations for polymer optoelectronic technologies. The Monte-Carlo analysis was carried out using Microsoft Excel with 10 000 random sampling iterations of the input distributions employed to calculate the probability distribution for C_{op}, E_{use} and $GHG\text{-}CO_{2,op}$.

The first scenario, assumes average luminous efficacy and operational lifetime values achievable using current small-scale production approaches, as reported in Table 3. The second scenario assumes "worst-case" luminous efficacy and operational lifetime values reported above due to large-scale production methods. The third scenario assumes a future "best case" scenario in which the luminous efficacy and operational lifetime values at large-scale production are 7.9 lm/W (same as currently-achievable small-scale production value) and 50 000 h (the operational lifetime of a commercial inorganic LED). Figure 6a shows that C_{op} was similar for small-scale and best-case, large-scale production at 94 $/a ± 33 $/a and was significantly lower than C_{op} for the worst-case, large-scale production (562 $/a ± 196 $/a), because C_{op} is inversely proportional to luminous efficacy and is insensitive to operational lifetime (as it is calculated on a yearly basis). However, E_{use}, is both inversely proportional to luminous efficacy

and directly proportional to operational lifetime. Therefore, the larger operational lifetime values for best-case, large-scale production resulted in larger E_{use} values (58 GJ ± 26 GJ) compared to the small-scale (33 GJ ± 14 GJ) and worst-case, large-scale production (21 GJ ± 9 GJ). In other words, a given device produced under the best-case, large-scale production scenario consumes significantly more energy than a device produced at small-scale or for the worst-cast, large-scale production scenario, simply because it operates for longer. However, $GHG\text{-}CO_{2,op}$ exhibited a similar trend to the C_{op} data as it is also calculated on a yearly basis (and, therefore, is independent of operational lifetime) with small-scale and best-case, large-scale production scenarios exhibiting the lowest emissions.

Based on these scenarios , it is hypothesized that P-OLEDs would have to be mass-produced with luminous efficacy and operational lifetime values reported for small-scale devices (Table 3) in order for them to be viable in terms of the metrics C_{op} and $GHG\text{-}CO_{2,op}$ and competitive with commercial inorganic LED counterparts. Luminous efficacy, in particular, is the more critical performance parameter to maintain upon scale-up since the yearly cost and energy to operate P-OLED devices and the yearly GHG-CO_2 emissions during operation are significantly greater than for the production of P-OLEDs even under the best-case, large-scale production scenario. For example, the projected best-case C_{op} (94 \$/a) and $GHG\text{-}CO_{2,op}$ (~1800 kg/a of CO_2) for top-emitting, inverted P-OLEDs fabricated using large-scale production are greater than the projected C_{dev} (~55 \$/m^2) and $GHG\text{-}CO_{2,dev}$ (~50 kg of CO_2) for large-scale production. Therefore, we expect that regular replacement of a P-OLED device would be relatively inexpensive and would have low greenhouse gas impacts - particularly in comparison to a commercial inorganic LED with similar luminous efficacy (C_{dev} of 844 \$/m^2 and $GHG\text{-}CO_{2,dev}$ of ~5000 kg of CO_2) - thereby making operational lifetime less critical. However, since processing techniques and manufacturing methods have not been standardized for P-OLEDs, it is difficult to draw definitive conclusions on what the projected device performance parameters should be for P-OLEDs upon scale-up. Therefore, studies such as ours would have to obtain performance parameter data from optimized large-scale production processes for P-OLEDs (which are still under development) and draw comparisons with

performance parameter data from existing optimized laboratory-scale or pilot-scale processes, which may result in currently unforeseen benchmarks [5]. Finally, it should be noted that for our study we focused only on blue light-emitting P-OLEDs and the metrics would most likely be improved for red and green P-OLEDs due to their higher efficiencies and longer operational lifetimes.

5.3. Conclusions

In conclusion, from a comparison of various P-OLEDs device architectures it was found that the top-emitting inverted P-OLED architecture is likely to be the most promising device architecture to pursue in terms of achieving operational lifetimes and efficiencies that are competitive with commercially-available blue inorganic LEDs and to achieving fully-solution processed large-scale production. Additionally, the device costs per area and embodied energies for the top-emitting P-OLEDs were significantly lower than those for the blue inorganic LED, making P-OLEDs already competitive in terms of up-front cost and energy expenditures. Given these factors and the performance parameters (luminous efficacy and operational lifetime) currently-achievable at lab-/prototype-scale, top-emitting P-OLEDs could be adopted for portable optoelectronic technologies (e.g., cell phone displays; indicator lights) due to the relatively short use stage of such technologies and inexpensive materials requirements that allow consumers to dispose of them after only 5-10 years. However, the performance parameters need to remain at current lab-/prototype-scale values during development and scale-up in order to ensure their performance is competitive with inorganic LEDs. Maintaining high luminous efficacy (i.e., electricity-to-light conversion efficiency) upon scale-up will be more important than maintaining long operational lifetimes, since the yearly cost and energy to operate P-OLED devices and the greenhouse gas emissions during operation are significantly greater than for the production of P-OLEDs. Therefore, regular replacement of a P-OLED device would be relatively inexpensive and would have low greenhouse gas impacts; particularly in comparison to an inorganic LED with similar luminous efficacy.

Acknowledgements

The authors gratefully acknowledge support from the Jerome Goldstein Scholarship Fund for EcoEntrepreneuring, the Corning, Inc. graduate fellowship program, Department of Education's Graduate Assistance in Areas of National Need (GAANN) fellowship program, National Science Foundation, Grant No. DMR-1309459, Rutgers' Institute for Advanced Materials Devices and Nanotechnology, Rutgers' Aresty Undergraduate Research Fellowship Program and The New Jersey Governor's School of Engineering and Technology Program. The authors thank Dr. Serpil Guran, Kelly Ruffenach, Sivarampragadeesh Siva and Xiaojun Wang for their support and useful interactions.

References

1. C. F. Wang et al (2013). Functionalized terfluorene for solution-processed high efficiency blue fluorescence OLED and electrophosphorescent devices. *Org. Electron.* **14**, 1958-1965.
2. D. Fyfe (2009). Organic displays come of age. *Nat. Photon.* **3**, 453-455.
3. F. So and D. Kondakov (2010). Degradation Mechanisms in Small- Molecule and Polymer Organic Light-Emitting Diodes. *Adv. Mater* **22**, 3762-3777.
4. C. J. M. Emmott, A. Urbina and J. Nelson (2012). Environmental and economic assessment of ITO-free electrodes for organic solar cells. *Sol. Energy Mater. Sol. Cells* **97**, 14-21.
5. S. Lizin et al (2013). Life cycle analyses of organic photovoltaics: a review. *Energy Environ. Sci.* **6,** 3136-3149.
6. S. B. Darling and F. You (2013). The case of organic photovoltaics. *RSC Adv.* **3**, 17633-17648.
7. U. S. Department of Energy (2012). Life-Cycle Assessment of Energy and Environmental Impacts of LED Lighting Products, Part I: Review of the Life-Cycle Energy Consumption of Incandescent, Compact Fluorescent, and LED Lamps. Solid-State Lighting Program. U.S. Department of Energy. Available from: http://apps1.eere.energy.gov/buildings/publications/pdfs/ssl/2012_LED_Lifecycle_Report.pdf (accessed February 2014).
8. P. de Bruyn, D. J. D. Moet and P. W. M. Blom (2012). All- solution processed polymer light-emitting diodes with air stable metal-oxide electrodes. *Org. Elect.* **13**, 1023-1030.

9. U. S. Department of Energy (2014). Solid-State Lighting Manufacturing Research and Development Roadmap. Available from: http://apps1.eere.energy.gov/buildings/publications/pdfs/ssl/ssl_mfg_roadmap_aug2014.pdf (accessed October 2015).
10. S. R. Tseng et al (2007). High-efficiency blue multilayer polymer light-emitting diode based on poly(9,9-dioctylfluorene). *J. Appl. Phys*. **101**, 084510 1-4.
11. R. Trattnig et al (2013). Bright Blue Solution Processed Triple-Layer Polymer Light-Emitting Diodes Realized by Thermal Layer Stabilization and Orthogonal Solvents. *Adv Func. Mat.* **23**, 4897-4905.
12. H. Zheng et al (2013). All-solution processed polymer light-emitting diode displays. *Nat. Commun.* 4:1971 doi:10.1038/ncomms2971,1-7.
13. V. Bodrozic et al (2008). The Built In Potential in Blue Polyfluorene-Based Light Emitting Diodes. *Adv. Mat.* **20**, 2410-2415.
14. H. Yan et al (2003). High-Brightness Blue Light-Emitting Polymer Diodes via Anode Modification Using a Self-Assembled Monolayer. *Adv. Mater.* **10**, 835-838.
15. T. M. Brown et al (1999). Built in field electroabsortion spectroscopy of polymer light-emitting diodes incorporating a doped poly(3,4-ethylene dioxythiophene) hole injection layer. *Appl. Phys. Lett*. **75**, 1679-1681.
16. C. C. Hsiao, A.E. Hsiao, and S.A. Chen (2008). Design of Hole Blocking Layer with Electron Transport Channels for High Performance Polymer Light-Emitting Diodes. *Adv. Mater.* **20,** 1982-1988.
17. T. M. Brown et al (2003). Electronic line-up in light-emitting diodes withalkali-halide/metal cathodes. *Appl. Phys. Lett*. **93**, 6159-6172.

693 18. E. L. William et al (2007). Excimer-based white phosphorescent organic light-emitting
694 diodes with nearly 100% internal quantum efficiency. *Adv. Mater*. ***19,*** 197-202.
695 19. S. Y. Kim and J. J. Kim (2010). Outcoupling efficiency of organic light emitting diodes
696 and the effect of ITO thickness. *Org. Electron.* **11**, 1010-1015.
697 20. C. F. Madigan, M. H. Lu and J. C. Sturm (2000). Improvement of output coupling
698 efficiency of organic light-emitting diodes by backside substrate modification. *Appl.*
699 *Phys. Lett.* **76**, 1650-1652.
700 21. X. Y. Deng (2011). Lighting- Emitting Devices with Conjugated Polymers. *Int. J. Mol.*
701 *Sci.* **12**, 1575-1594.
702 22. S. H. Chen and S. C. Chan (2012). Light Enhancement of Plasmonic Nanostructures for
703 Polymer Light-Emitting Diodes at Different Wavelengths. *Appl. Phys. Express* **5**,
704 062001-1-3.
705 23. X. H. Li et al (2012). Efficient Inverted Polymer Solar Cells with Directly Patterned
706 Active Layer and Silver Back Grating. *J. Phys. Chem. C* **116**, 7200-7206.
707 24. J. Zhong et al (2012). Effect of Encapsulation Technology on Organic Light Emitting
708 Diode Lifetime. *Opt. Rev*. **19**, 82-85.
709 25. M. F. Ashby (2013). Materials and the Environment. Butterworth-Heinemann 2nd edition.
710 26. T Swarr et al (2011) Environmental life cycle costing: a code of practice. SETAC Press,
711 Pensacola, ISBN 978-1-880611- 87-6.
712 27. N. Espinosa and F. C. Krebs (2014). Life cycle analysis of organic tandem solar
713 cells:When are they warranted? *Sol. Energy Mater. Sol. Cells*. **120**, 692-700.
714 28. L. Tähkämö et al (2013). Life cycle assessment of light-emitting diode downlight
715 luminaire - a case study. *Int. J. Life Cycle Assess.* **18**, 1009-1018.

29. D. Yue et al (2012). Deciphering the uncertainties in life cycle energy and environmental analysis of organic photovoltaics. *Energy Environ. Sci.* **5**, 9163-9172.

30. R. Garcı´a-Valverde, J. A. Cherni and A. Urbina (2010). Life cycle analysis of organic photovoltaics. *Prog. Photovolt: Res. Appl.* **18**, 535-558.

31. N. Espinosa et al (2011). A life cycle analysis of polymer solar cell modules prepared using roll-to-roll methods under ambient conditions. *Sol. Energy Mater. Sol. Cells* **95**, 1293-1302.

32. B. Azzopardi et al (2011). Economic Assessment of Solar Electricity Production from Organic-Based Photovoltaic Modules In A Domestic Environment. *Energy Environ. Sci*. **4**, 3741-3753.

33. Anctil et al (2012). Cumulative energy demand for small molecule and polymer photovoltaics. *Prog. Photovolt.: Res. Appl*. **21**, 1541-1554.

34. Y.S. Zimmerman et al. (2012). Organic photovoltaics: Potential fate and effects in the environment. *Environ. Int.* **49**, 128-140.

35. C. Kapnopoulos et al (2016). Fully gravure printed organic photovoltaic modules: A straightforward process with a high potential for large scale production. *Sol. Energy Mater. Sol. Cells* **144**, 724-731.

36. M. T. Llyod et al. (2011). Influence of the hole-transport layer on the initial behavior and lifetime of inverted organic photovoltaics. *Sol. Energy Mater. Sol. Cells* **95**, 1382-1388.

37. Y. L. Powell and T. Bender (2012). Using stochastic model to determine financial indicator and technical objectives for organic solar cells. *Sol. Energy Mater. Sol. Cells* **107**, 236-247.

738 38. C. J. Mulligan et al (2014). A projection of commercial scale organic photovoltaic
739 module costs. *Sol. Energy Mater. Sol. Cells* **120**, 9-17.
740 39. J. Schmidtke (2010). Commercial status of thin-film photovoltaic devices and materials.
741 *Opt. Express* **18**, A477-A486.
742 40. E. Alsema (1998). Energy requirements of thin-film solar cell modules - a review.
743 *Renew. Sustain. Energy Rev.* **2**, 387-415.
744 41. International Organization for, Standardization, ISO 14040 series. Environmental
745 management - life cycle assessment, 2006.
746 42. H. Bauman and A.M. Tillman (2004). The Hitch Hiker's Guide to LCA. Studentlitteratur
747 AB, Lund, ISBN-10:9144023642.
748 43. J. H. Youn, S. J. Baek, H. P. Kim, D. H. Nam, Y. Lee, J. G. Leeb, J. Jang (2013).
749 Improving the lifetime of a polymer light-emitting diode by introducing solution
750 processed tungsten oxide. *J. Mater. Chem. C* **1**, 3250.
751 44. M. Roberts, N. Akino, K. Asada, P. Benzie, H. Hamamatsu, M. Hatcher, S. King, E.
752 Snedden, A. Strevens, S. Tanaka, J. Toner, R. Wilson, W. Young, K. Yamamoto, T.
753 Yamada (2013). High efficiency Polymer OLEDs - analysis and progress. *SPIE Opt.*
754 *Photon.* 2013 https://www.cdtltd.co.uk/pdf/spie2013-mroberts-cdt.pdf (accessed
755 February 2016).
756 45. T. -Y. Chu, J. -F. Chen, S. -Y. Chen, C. -J. Chen, C. H. Chen (2006). Highly efficient and
757 stable inverted bottom-emission organic light emitting devices. *Appl. Phys. Lett.* **89**,
758 053503.

759 46. S. -Y. Chen, T. -Y. Chu, J. -F. Chen, C. -Y. Su, C. H. Chen (2006). Stable inverted
760 bottom-emitting organic electroluminescent devices with molecular doping and
761 morphology improvement. *Appl. Phys. Lett.* **89**, 053518.
762 47. D. Fyfe (2009). Organic displays come of age. *Nat. Photon*. **3**, 453-455.
763 48. E. Fred Schubert, *Light-Emitting Diodes*, Chapter 16, Cambridge University Press,
764 Cambridge, UK (2006).
765 49. N. Na, J. Jang and H.-J. Suk (2014). Dynamics of Backlight Luminance for Using
766 Smartphone in Dark Environment, *Proc. of SPIE* **9014**, 90140I-1-6.
767 50. M. H. Chang et al (2012). Light emitting diodes reliability review. *Microelec. Reliability*
768 **5**, 762-782.
769 51. Joint Research Centre of the European Commission (2012). International Reference Life
770 Cycle Data System (ILCD) Handbook, General Guide for Life Cycle Assessment,
771 detailed guidance, Joint Research Centre, Institute for Environment and Sustainability,
772 Publications Office of the European Union, Luxembourg, 2010. Available from:
773 http://publications.jrc.ec.europa.eu/repository/bitstream/JRC48157/ilcd_handbook-
774 general_guide_for_lca-detailed_guidance_12march2010_isbn_fin.pdf (accessed May
775 2016).
776 52. A. Kohler and H. Bassler (2015). Electronic Processes in Organic Semiconductors: An
777 Introduction. Wiley Press, ISBN: 978-3-527-33292-2.
778 53. B. D. Chin et al (2004). Effects of cathode thickness and thermal treatment on the design
779 of balanced blue light-emitting polymer device. *Appl. Phys. Lett.* **85**, 4496-4498.
780 54. H. J. Bolink et al (2007). Air stable hybrid organic-inorganic light emitting diodes using
781 ZnO as the cathode. *Appl. Phys. Lett*. **91**, 223501-1-3.

55. C. Y. Wu et al (2010). Flexible inverted bottom-emitting organic light-emitting devices with semi-transparent metal-assisted electron-injection layer. *J. Soc. Info. Display* **18**, 76-80.

56. W. Liu et al (2014). Efficient inverted organic light-emitting devices with self or intentionally Ag-doped interlayer modified cathode. *Appl. Phys. Lett.* **104**, 0993305-1-4.

57. J. Liu et al (2014). Achieving above 30% external quantum efficiency for inverted phosphorescence organic light-emitting diodes based on ultrathin emitting layer. *Org. Electron.* **15**, 2492-2498.

58. X. W. Zhang et al (2012). A very simple method of constructing efficient inverted top-emitting organic light-emitting diode based on Ag/Al bilayer reflective cathode. *J. Luminesce.* **132**, 1-5.

59. K. A. Knauer et al (2012). Inverted top-emitting blue electrophosphorescent organic light-emitting diodes with high current efficacy. *Appl. Phys. Lett.* **101**, 103304-1-4.

60. S. Hofle et al (2014). Solution processed, white emitting tandem organic light-emitting diodes with inverted device architecture. *Adv. Mater.* **26**, 5155-5159.

61. J. Chem (2012). Solution-processable small molecules as efficient universal bipolar host for blue, green, and red phosphorescent inverted OLEDs. *J. Mater. Chem.* **22**, 5164-5170.

62. Super Bright LEDs Inc., Super-Blue LED (InGaN), Part Number: RL5-B55a5, https://www.superbrightleds.com/moreinfo/through-hole/5mm-blue-led-15-degree-viewing-angle-5500-mcd/269/ (accessed May 2016).

63. JKL Components Corp., T-1 3/4 Wedge Base 12 Volt LED, Part Number LE-0504-01B, http://www.jkllamps.com/led/wedgebaseleds (accessed May 2016).

804 64. TAIWAN HongGuang 3W RGB LED Emitter (white) (distributed by Fancy Cost, Item
805 Code 1068112); only specifications for the blue LED component used in this study.
806 65. CREE, Inc., Xlmap MC-E RGBW (http://www.cree.com/LED-Components-and-
807 Modules/Products/XLamp/Arrays-Directional/XLamp-MCE, accessed May 2016); only
808 specifications for the blue LED component was used in this study.
809 66. O. V. Mikhnenko, P. W. M. Blom and T. Q. Nguyen (2015). Exciton diffusion in organic
810 semiconductors, *Energy Environ. Sci*. **8**, 1867-1888.
811 67. Euro to dollar conversion factor of 1.35 was employed as of November 2013.
812 68. N.Narendran et al. (2004) Solid- state lighting: Failure analysis of white LEDs. *J. Cryst.*
813 *Grow.* **268**, 449-456.
814 69. State Electricity Profile 2010. DOE/EIA-0348(01)/2. Released January 27, 2012.
815 http://www.eia.gov/electricity/state/pdf/sep2010.pdf (accessed October 2015).
816 70. J. A. deGouw et al. (2014). Reduced emissions of CO2, NOx, and SO2 from U.S. power
817 plants owing to switch from coal to natural gas with combined cycle technology. *Earth's*
818 *Future*, **2**, 75-82, doi:10.1002/2013EF000196.
819 71. M. Lu, P. Bruyn, H. T. Nicolai and G. J. Wetzelaer (2012). Hole-enhanced electron
820 injection from ZnO in inverted polymer light-emitting diodes. *Org. Elect.* **13**, 1693-1699.
821 72. V. N. Bliznyuk et al (1999). Electrical and Photoinduced Degradation of Polyfluorene
822 Based Films and Light Emitting Devices. *Macromol*. **32**, 361-369.
823 73. S. A. Choulis et al (2005). The effect of interfacial layer on the performance of organic
824 light emitting diodes. *Appl. Phys. Lett.* ***87***, 113503-1-3.
825 74. D. Kasama et al (2009). Improved Light Emission Utilizing Polyfluorene Derivatives by
826 Thermal Printing and Solution Process. *Proc. SPIE.* ***7415***, 74151N 1-7.

827 75. Q. Zhao, S.J. Liu and W. Huang (2009). Polyfluorene-Based Blue-Emitting Materials.
828 *Macro. Chem. Phys.* **210**, 1580-1590.
829 76. T. F. Guo et al (2001). High Performance Polymer Light- Emitting Diodes Fabricated by
830 a Low Temperature Lamination Process. *Adv. Funct. Mat*. **11**, 339- 343.
831 77. H. J. Bolink et al (2008). Inverted Solution Processable OLEDS using a metal oxide as
832 electron injection contact. *Proc. of SPIE* **6999**, 69992X1-69992X11.
833 78. H. Choi et al (2011). Combination of Titanium Oxide and a Conjugated Polyelectrolyte
834 for High-Performance Inverted Type Organic Optoelectronic Devices. *Adv. Mater.* **23**,
835 2759-2763.
836 79. D. Kabra et al (2010). Efficient Single Layer Polymer Light Emitting Diodes. *Adv.*
837 *Mater.* **22**, 3194-3198.
838 80. F. So and D. Kondakov (2010). Degradation Mechanisms in Small- Molecule and
839 Polymer Organic Light-Emitting Diodes. *Adv. Mater.* **22**, 3762-3777.
840 81. X. H. Li et al (2012). Efficient Inverted Polymer Solar Cells with Directly Patterned
841 Active Layer and Silver Back Grating. *J. Phys. Chem. C* **116**, 7200-7206.
842 82. H. J. Bolink et al (2010). Phosphorescent Hybrid Organic-Inorganic Light-Emitting
843 Diodes. *Adv. Mater*. **2**, 2198-2201.
844 83. S. N. Hsieh et al (2009). Surface modification of TiO2 by a self-assembly monolayer in
845 inverted-type polymer light emitting devices. *Org. Elect*. **10**, 1626-1631.
846 84. J. S. Park et al (2011). High performance polymer light-emitting diodes with n-type metal
847 oxide/conjugated polyelectrolyte hybrid charge transport layers. *Appl. Phys. Lett.* **99**,
848 163305-1-4.

85. X. W. Zhang et al (2013). Improving electron injection and microcavity effect for constructing highly efficient inverted top-emitting organic light-emitting diode. *Opt. Laser Technol.* **45**, 181-184.

86. Y. Y. Zhang and Y. A. Yin (2011). Performance enhancement of blue light-emitting diodes with a special designed AlGaN/GaN superlattice electron-blocking layer. *Appl. Phys. Lett.* **99**, 221103.

87. R. Dahal, C. Ugolini, J. Y. Lin, H. X. Jiang, J. M. Zavada (2010). 1.54 μm emitters based on erbium doped InGaN p-i-n junctions. *Appl. Phys. Lett.* **97**, 141109.

88. Ted Pella, Inc. "Glass Microscope Slide" http://www.tedpella.com/histo_html/slides.htm (accessed November 2012).

89. S. Xiao et al (2005). Effects of Solvent on Fabrication of Polymeric Light Emitting Devices. *Mat. Lett.* **59**, 694-696.

90. *Heraeus Clevios,"Printing Conductivity"* <http://www.heraeus-clevios.com/media/webmedia_local/media/technical_informations___flyer/document_HCS_Flyer_CLEVIOS_Printing.pdf> (accessed November 2012).

91. *Sigma Aldrich* "655201 - Poly(3,4-ethylenedioxythiophene)-poly(styrenesulfonate)" http://www.sigmaaldrich.com/catalog/product/aldrich/655201?lang=en&region=US (accessed October 2013).

92. Sigma Aldrich. "571652 - Poly(9,9-di-n-octylfluorenyl-2,7-diyl)"*http://www.sigmaaldrich.com/catalog/product/aldrich/571652?lang=en&region=US* (accessed October 2013).

870 93. Sigma Aldrich. “449903 - Lithium fluoride”
871 *http://www.sigmaaldrich.com/catalog/product/aldrich/449903?lang=en&region=US*
872 (accessed October 2013).
873 94. Sigma Aldrich “266523 - Aluminum”
874 *http://www.sigmaaldrich.com/catalog/product/sial/266523?lang=en&region=US*
875 (accessed October 2013).
876 95. Sigma Aldrich. “204757 - Titanium(IV) oxide”
877 http://www.sigmaaldrich.com/catalog/product/aldrich/204757?lang=en&region=US
878 (accessed October 2013).
879 96. Sigma Aldrich. “203815 - Molybdenum(VI) oxide”
880 http://www.sigmaaldrich.com/catalog/product/aldrich/203815?lang=en&region=US
881 (accessed October 2013).
882 97. Sigma Aldrich. “327050 - Silver”
883 http://www.sigmaaldrich.com/catalog/product/aldrich/327050?lang=en&region=US
884 (accessed October 2013).
885 98. O. Tsydenova and M. Bengtsson (2011). Chemical hazards associated with treatment of
886 waste electrical and electronic equipment. *Waste Manage.* **31**, 45-58.
887 99. J. D. Lincoln et al (2007). Leaching Assessments of Hazardous Materials in Cellular
888 Telephones. *Environ. Sci. Technol.* **41**, 2572-2578.
889 100. http://minerals.usgs.gov/minerals/pubs/commodity/recycle/recymyb01.pdf
890 101. R. Geyer and V. D. Blass (2010). The economics of cell phone reuse and
891 recycling. *Int. J Adv. Manuf. Technol.* **47**, 515-525.

892 102. B. H. Robinson (2009). E-waste: An assessment of global production and
893 environmental impacts. *Sci. Total Environ.* **408**, 183-191.
894 103. J. L. Sullivan and L. Gaines (2012). Status of life cycle inventories for batteries.
895 *Energy Convers. Manage.* **58**, 34-148.
896 104. G. P. Hammond and C. I. Jones (2008). Embodied energy and carbon in
897 construction materials. *Proc. Inst. Civil Eng. - Energy* **161**, 87-98.
898 105. G.F. Grubb and B.R. Bakshi (2010). Life Cycle of Titanium Dioxide Nanoparticle
899 Production. *J. Ind. Ecol.* **15,** 81-95.
900 106. N. Osterwalder et al (2006). Energy consumption during nanoparticle production:
901 How economic is dry synthesis? *J. Nanopart. Res.* **8**, 1-9.
902 107. S. J. Hong, *Characteristics of Indium Tin Oxide (ITO) Glass Re-Used from Old*
903 *TFT-LCD Panel.* Available from https://www.jim.or.jp/journal/e/pdf3/53/05/968.pdf
904 (accessed June 2016).
905 108. V. Zardetto, T. M. Brown, A. Reale, A. Di Carlo (2011). Substrates for Flexible
906 Electronics: A Practical Investigation on the Electrical, Film Flexibility, Optical,
907 Temperature, and Solvent Resistance. *J. Poly. Sci. Part B: Poly. Phys.* **49**, 638-648.
908 109. ARENA (2014). Market Technology Analysis Lessons Learnt. Australian
909 Renewable Energy Agency. Available from: http://arena.gov.au/files/2014/06/Market-
910 Technology-Analysis_-Lessons-Learnt.pdf (accessed May 2016).
911 110. F. C. Krebs, N. Espinosa, M. Hösel , R. R. Søndergaard, M. Jørgensen (2014).
912 25th Anniversary Article: Rise to Power - OPV-Based Solar Parks. *Adv. Mater.* **26**, 29-
913 39.

111. M. Corazza, F. C. Krebs, S. A. Gevorgyan (2015). Lifetime of organic photovoltaics: Linking outdoor and indoor tests. *Sol. Energy Mater. Sol. Cells* **143**, 467-472.

112. C. J. M. Emmott, D, Moia, P. Sandwell, N. Ekins-Daukes, M. Hösel, L. Lukoschek, C. Amarasinghe, F. C. Krebs, J. Nelson (2016). In-situ, long-term operational stability of organic photovoltaics for off-grid applications in Africa. *Sol. Energy Mater. Sol. Cells* **149**, 284-293.

113. P. Kumar, C. Bilen, B. Vaughan, X. Zhou, P. C. Dastoor, W. J. Belcher (2016). Comparing the degradation of organic photovoltaic devices under ISOS testing protocols. *Sol. Energy Mater. Sol. Cells* **149**, 179-186.

114. Z. Ding, J. Kettle, M. Horie, S. W. Chang, G. C. Smith, A. I. Shames, E. A. Katz (2016). Efficient solar cells are more stable: the impact of polymer molecular weight on performance of organic photovoltaics. *J. Mater. Chem. A* **4**, 7274.

115. S. A. Gevorgyan, M. V. Madsen, B. Roth, M. Corazza, M. Hösel, R. R. Søndergaard, M. Jørgensen, F. C. Krebs (2016). Lifetime of Organic Photovoltaics: Status and Predictions. *Adv. Energy Mater.* **6**, 1501208.

116. C. H. Peters, I. T. Sachs-Quintana, J. P. Kastrop, S. Beaupré, M. Leclerc, M. D. McGehee (2011). High Efficiency Polymer Solar Cells with Long Operating Lifetimes. *Adv. Energy Mater.* **1**, 491-494.

117. T. T. Larsen-Olsen, et al. (2013). A round robin study of polymer solar cells and small modules across China, *Sol. Energy Mater. Sol. Cells* **117**, 382-389.

118. A. M. Nardes, C. L. Perkins, P. Graf, J. V. Li, S. E. Shaheen, D. Ostrowski, A. Watte, D. C. Olson, N. Kopidakis (2014). Thermal annealing affects vertical morphology,

doping and defect density in BHJ OPV devices. *40th IEEE Photovoltaic Specialist Conference (IEEE-PVSC)* 2575-2580.